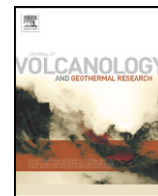




Contents lists available at SciVerse ScienceDirect

Journal of Volcanology and Geothermal Research

journal homepage: www.elsevier.com/locate/jvolgeores

Rapid changes in magma storage beneath the Klyuchevskoy group of volcanoes inferred from time-dependent seismic tomography

Ivan Koulakov^{a,*}, Evgeniy I. Gordeev^b, Nikolay L. Dobretsov^a, Valery A. Vernikovskiy^a, Sergey Senyukov^c, Andrey Jakovlev^a, Kayrly Jaxybulatov^a^a Institute of Petroleum Geology and Geophysics, SB RAS, Novosibirsk, Russian^b Institute of Volcanology and Seismology FEB RAS, Petropavlovsk-Kamchatsky, Russia^c Kamchatka Branch of Geophysical Survey, RAS, Petropavlovsk-Kamchatsky, Russia

ARTICLE INFO

Article history:

Received 26 December 2011

Accepted 22 October 2012

Available online xxxxx

Keywords:

Seismic tomography

Klyuchevskoy volcano

Magma sources

Kamchatka

ABSTRACT

We present the results of time-dependent local earthquake tomography for the Klyuchevskoy group of volcanoes in Kamchatka, Russia. We consider the time period from 1999 to 2009, which covers several stages of activity of Klyuchevskoy and Bezmianny volcanoes. The results are supported by synthetic tests that recover a common 3D model based on data corresponding to different time windows. Throughout the period, we observe a robust feature below 25 km depth with anomalously high V_p/V_s values (up to 2.2). We interpret this feature as a channel bringing deep mantle materials with high fluid and melt content to the bottom of the crust. This mantle channel directly or indirectly determines the activity of all volcanoes of the Klyuchevskoy group. In the crust, we model complex structure that varies over time. During the pre-eruptive period, we detected two levels of potential magma storage: one in the middle crust at 10–12 km depth and one close to the surface just below Klyuchevskoy volcano. In 2005, a year of powerful eruptions of Klyuchevskoy and Besmianny volcanoes, we observe a general increase in V_p/V_s throughout the crust. In the relaxation period following the eruption, the V_p/V_s values are generally low, and no strong anomalous zones in the crust are observed. We propose that very rapid variations in V_p/V_s are most likely due to abrupt changes in the stress and deformation states, which cause fracturing and the active transport of fluids. These fluids drive more fracturing in a positive feedback system that ultimately leads to eruption. We envision the magma reservoirs beneath the Klyuchevskoy group as sponge-structured volumes that may quickly change the content of the molten phases as fluids pulse rapidly through the system.

© 2012 Elsevier B.V. All rights reserved.

1. Introduction

Since ancient times, people have sought to understand the behavior and mechanics of volcanic eruptions. Our generation has the chance to make a breakthrough in this direction. In the last few decades, the rapid development of geophysical observations and algorithms has made it possible to image volcanic interiors and to reconstruct volcanic processes. Even so, the mechanics of volcanism are far from being well understood. For example, magma reservoirs beneath volcanoes, which are often described by over-simplified cartoons, are not simple objects that can be easily detected by geophysical tools, and thus their existence is not definitively proven. Popular Hollywood movies may present scenarios showing the temporal evolution of real-time 3D images of bodies beneath volcanoes, but unfortunately, the real capabilities of the present-day science are far more limited.

Joint analysis of geological, geophysical and petrological data shows that the feeding mechanisms beneath volcanoes may be very complex. This is evidenced by the strong spatial variations in composition and eruptive style that can exist even within tightly clustered groups of volcanoes. (e.g., Laverov, 2005; Khubunaya et al., 2007). Often, considerable changes may occur in one volcanic complex during a relatively short period of time (e.g., Khrenov et al., 1989; Vlastélic et al., 2005). Monitoring physical parameters beneath volcanoes has shown that eruption processes can cause rapid changes (days to years) in the deep structure beneath volcanoes (e.g., Vlastélic et al., 2005; Hoffmann-Rothe et al., 2006; Wegler et al., 2006). One of the most powerful methods for imaging deep structure, seismic tomography, can also be of great use for observing time-varying structure. Recently, there has been some success in studying temporal variations using earthquake tomography (e.g., Julian and Foulger, 2010). However, there has been only one published study of temporal evolution of 3D seismic structure beneath a volcano (Mt. Etna) of which the authors are aware (Patanè et al., 2006). Recently there have been successful attempts to observe the temporal variations of seismic anisotropy derived from shear wave splitting (Savage et al., 2010a) and to link them with changing stress states in volcanoes and GPS observations (Savage et al., 2010b).

* Corresponding author. Tel.: +7 9134538987.

E-mail addresses: koulakovI@ipgg.nsc.ru (I. Koulakov), gordeev@kscnet.ru (E.I. Gordeev), VernikovskiyVA@ipgg.nsc.ru (V.A. Vernikovskiy), ssl@emsd.iks.ru (S. Senyukov), jakovlevAV@ipgg.nsc.ru (A. Jakovlev).

A number of previous tomographic studies provide a multi-scale view on the processes beneath the Kluchevskoy group and the surrounding areas. The structure of the upper mantle has been investigated in regional tomographic studies based on global body and surface wave data (e.g., [Gorbatov et al., 2001](#); [Levin et al., 2002](#); [Lees et al., 2007a](#); [Koulakov et al., 2011a](#)). These results show that the horizontal distance from the volcanic group to the edge of the subducting Pacific plate is less than 100 km, whereas the vertical distance to the upper surface of the plate is approximately 150 km. The structure above the subducting slab beneath the Kamchatka peninsula has been studied based on travel times from seismicity in the Benioff zone recorded by regional networks ([Gorbatov et al., 1999](#); [Nizkous et al., 2006](#)). Local structures beneath the Kluchevskoy group, using similar ray configurations as this study, have been investigated in a number of tomography studies (e.g., [Slavina et al., 2001](#); [Lees et al., 2007b](#); [Nizkous et al., 2007](#); [Koulakov et al., 2011b](#)) and more recently with receiver function techniques ([Nikulin et al., 2010](#); [Nikulin et al., 2012](#)). The work by ([Koulakov et al., 2011b](#)) was performed for a dataset corresponding to one year in 2004 using the same tomographic algorithm as in this study. It reveals a complex crustal structure with multi-level magma sources, likely responsible for feeding magma to the volcanoes of the group. None of the mentioned tomographic studies considered temporal variation, however, its potentially important role was mentioned in [Koulakov et al. \(2011b\)](#).

In this paper, we present a 4D tomographic model beneath the Kluchevskoy volcanic group that shows not only the spatial heterogeneities of seismic parameters, but also their temporal evolution. We consider the time period from 1999 to 2009, which covers different stages of the activity of Kluchevskoy and Bezmianny volcanoes: pre-eruption, eruption, and relaxation.

2. Study area

The study area includes the Kluchevskoy group of volcanoes on the Kamchatka peninsula in the Russian far east. This isolated group is located at the northeast corner of the subducting Pacific plate ([Fig. 1A](#)). It includes active and dormant volcanoes, three of which (Kluchevskoy, Tolbachik and Bezmianny) are among the most productive and active volcanoes in the world. The namesake of the group, Kluchevskoy, has an elevation exceeding 4800 meters and is the largest active volcano in continental Eurasia ([Laverov, 2005](#)). An interesting feature of the Kluchevskoy group is its range in composition and eruptive styles ranging from explosive andesitic to fissure basalt Hawaiian-type eruptions (e.g., [Fedotov et al., 2010](#)). There is clear evidence at some volcanoes in the group that the eruptive styles and composition changed abruptly over short periods of time ([Laverov, 2005](#)). This diversity in space and time indicates that feeding of the volcanoes may occur both directly from mantle sources and through a complex system of intermediate magma sources in the crust ([Ozerov et al., 1997, 2007](#); [Khubunaya et al., 2007](#)). Another feature of this region that is very important for tomographic inversion is that most seismic events occur at depths between 23 and 33 km ([Fig. 2E](#)). This is a rare situation that allows the crust to be “illuminated” from below providing much better seismic ray coverage for tomographic inversion than is possible at most volcanoes (e.g., [Patanè et al., 2006](#)).

The study period from 1999 to 2009 covers different stages of activity at Kluchevskoy ([Ivanov, 2008, Fig. 2B](#)). Before 2003, Kluchevskoy remained relatively quiescent. In 2003, moderate levels of activity were observed probably resulting from upwelling magma. A relatively quiet period in 2004 corresponds to the preparation of a new stage of eruptive activity that occurred in the beginning of 2005. In the following

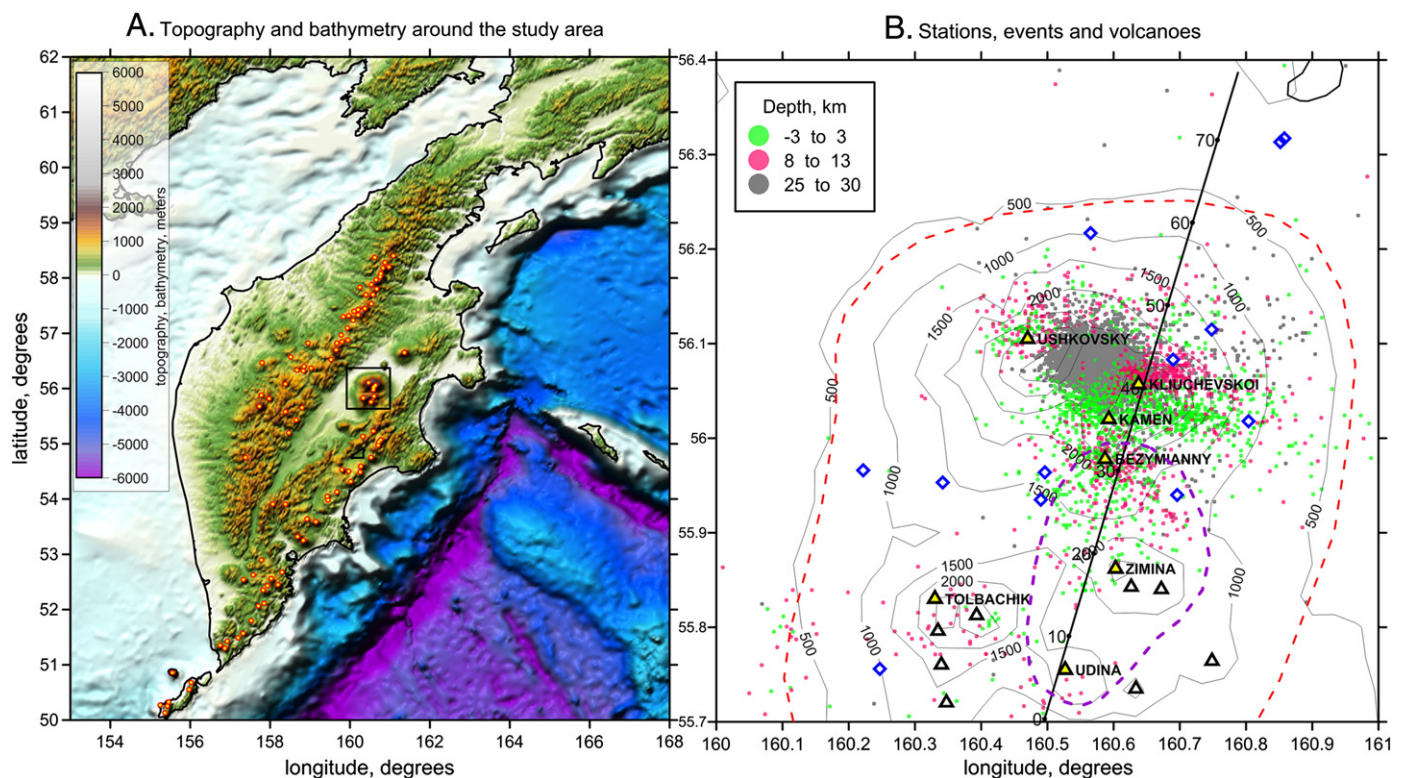


Fig. 1. A: Topography and bathymetry around the Kamchatka Peninsula. Circles indicate Holocene volcanoes. The location of the study area is marked by the square. B: Study area, earthquakes, and seismic stations. Contour lines show the smoothed relief; blue diamonds depict seismic stations; yellow and open triangles mark the locations of the main volcanoes and additional craters; the profile for presenting the main results is shown by the black line. Seismicity is colored in three depth intervals, corresponding to the three levels of magma sources observed in this study. Violet dotted line highlights the region of dacite-andesite volcanic products; red dotted line includes the region of basaltic and andesite-basaltic volcanism. (For interpretation of the references to color in this figure legend, the reader is referred to the web version of this article.)

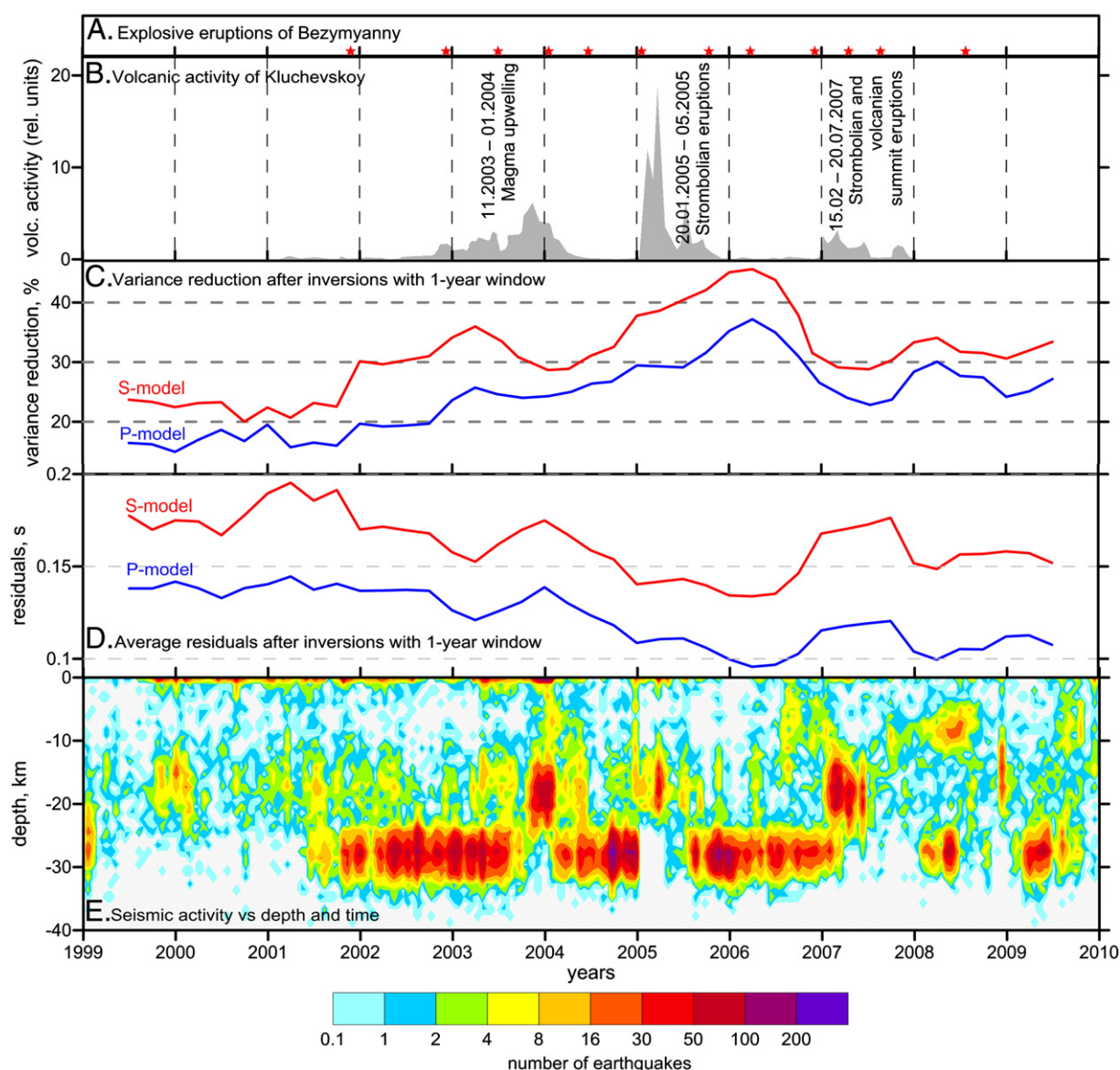


Fig. 2. Analysis of the time distribution of volcanic activity, seismicity and data quality. A) Explosive eruptions of Bezmyanny volcano marked with red stars. B) Kluchevskoy volcano activity (composite index including seismicity, fumarole and lava eruptions proposed by Ivanov, 2008). C and D) Variance reduction and RMS of travel time residuals, respectively, for the final models computed in 40 overlapping yearly time windows. E) The distribution of seismicity in the study area versus the depth and time. (For interpretation of the references to color in this figure legend, the reader is referred to the web version of this article.)

years, Kluchevskoy experiences intermittent periods of quiescence and eruption. Note that the seismicity variations in Fig. 2E correlate with eruptive periods at Kluchevskoy. In particular, gaps in deep seismicity between 23 and 33 km depth correspond to the periods of the volcanic activity. There is evidence that these gaps are real and not due to noisy periods of data that might limit the ability to record earthquakes in this depth range (Senyukov et al., 2009).

During the study period, another volcano of the group, Bezmyanny, which is an explosive andesite volcano consisting of 54.5% to 62.5% SiO_2 (Gorshkov and Bogoyavlenskaya, 1965; Ozerov et al., 1997), showed activity that is considerably different than Kluchevskoy. Eruptions at Bezmyanny (Fig. 2A) occur rather regularly (one to two times per year) as moderate explosions causing ash plumes that reach altitudes of 7 to 10 km. These eruptions are usually fairly brief (from a few hours to several days). The seismicity beneath Bezmyanny is much weaker than seismicity beneath Kluchevskoy. The eruptions at Bezmyanny are often coincident with the activity of Kluchevskoy.

For example, in the study period, the strongest (VEI-2) eruption of Bezmyanny occurred on 11 January 2005, almost simultaneously with the beginning of the most intensive eruption of Kluchevskoy. Though these volcanoes are separated by 8 km and have different eruption styles, the concurrence of these eruptions further suggests that the two systems are intimately linked at depth.

3. Data and algorithms

In this study, we use a very large dataset that includes more than 500,000 travel times from approximately 80,000 local earthquakes recorded from January 1999 to December 2009. These data were recorded at 17 stations from the permanent network run by the Kamchatka Branch of the Geophysical Survey of the Russian Academy of Sciences (Fig. 1B). All the stations after the year 2000 were equipped with digital three-component seismometers of various marks (mostly, short-period sensors with the periods of up to 1 s). For most events,

both P- and S-picks were detected, resulting in an approximately equal number of P and S data. The relatively small number of stations is compensated by a large number of events and their broad distribution. For time-lapse tomography, it is important that these data are uniformly distributed over the study period. Further uniformity of the data distribution was achieved by additional earthquake selection procedure. Based on the catalog location of events we analysed their distributions in a regular grid of $0.5 \times 0.5 \times 0.5$ km boxes. For each time period we subset a predefined number of events in each cell (from 3 to 10, depending on the year) having the maximum number of recorded picks. We did not use magnitude in a selection criterion; instead we fixed the minimum number of recorded phases per event at 9. The events with smaller number of phases appear to be useless for tomography and were not used for further analysis. After this selection process, 4000 to 6000 earthquakes per year were used (Fig. 2E). The total number of picks per year varied from 50,000 to 80,000; the number of P and S picks were approximately equal.

Roughly the same dataset has been used by previous authors (Slavina et al., 2001; Nizkous et al., 2006; Khubunaya et al., 2007), who reported P-wave velocities beneath the Kluchevskoy group. We also performed a single velocity inversion for the full dataset and have obtained similar results to the previous studies. However, the rather small variance reduction (about 15%) makes us doubt the robustness of this velocity solution due to its inability to fit all the data well. This was supported by our previous study (Koulakov et al., 2011b) in which we performed an inversion for one year of data (2004) and obtained a much more robust solution than for inversion of the entire dataset.

The main result of this study is a series of tomographic models obtained for data in a moving time window. We found that the optimal length of the window is one year, which utilises a sufficient amount of data for good coverage, but is short enough to resolve temporal variations. To explore the effect of temporal variations, we performed 40 inversions in overlapping one-year windows with three-month steps. In this paper, we focus our results and discussion on the calendar years 2001 through 2008. Before 2001, several stations did not yet exist resulting in poor ray coverage.

We use the LOTOS algorithm for local earthquake tomography (Koulakov, 2009), which performs iterative simultaneous inversions for P and S velocity and source parameters. The V_p/V_s values are derived from the independent P- and S-velocities. Some authors (e.g., Graeber and Asch, 1999) argue that this approach provides less stable results for V_p/V_s than direct inversion for V_p and V_p/V_s parameters. In the next section we present arguments in favor of the first scenario based on synthetic modelling.

We use the same 1D starting model for all time periods to help minimise variations in the inversion process. This 1D model (P and V_p/V_s) was selected because it provided the best fit (minimum RMS travel time misfit) to a subset of the highest quality earthquake solutions. This test did not assume fixed earthquake solutions. As in the 3D inversions, hypocentral locations were allowed to vary in the inversions. The model, given in Table 1, determines values of P-velocity at different depth levels and a constant V_p/V_s ratio equal to 1.75. Between the

depth levels, the velocity is linearly interpolated. This was used as the reference starting model for all 3D inversions.

The LOTOS code uses an adaptive mesh parameterisation with nodes distributed inside the study volume according to the ray sampling. No nodes are created in areas with insufficient ray coverage (less than 10% of average ray density). In visualisations, the results are masked if the distance to the nearest node is less than a predefined value (5 km in our case). The minimal grid spacing is predefined (2 km in our case). To avoid any artifacts related to grid orientations, we performed the calculations for four different versions of the mesh oriented at different geographic bearings (0° , 22° , 45° , and 67°). The results of these four inversions are then merged into a single model.

Each iteration within the LOTOS workflow consists of three major steps: (i) location of the earthquakes in the most up-to-date version of the model; (ii) calculation of the first derivative matrix; and (iii) inversion using the LSQR algorithm (Paige and Saunders, 1982). Five iterations were performed for all time periods. Increasing the number of iterations has a similar effect as decreasing the damping value. Five iterations provided a compromise between computational cost and the minimisation of non-linear effects. The values of damping (smoothing and amplitude regularisation) were selected based on synthetic tests with realistic data and noise distributions.

When performing 4D tomography, some authors (e.g., Julian and Foulger, 2010) propose applying smoothing over time. This approach appears reasonable as it compensates for a lack of data in some time periods. This ensures similarity of the results in neighboring time periods and makes the tomographic time series more continuous. At the same time, automatically applying this approach may be risky. It may hide actual rapid changes in the structure, and it requires additional user-defined parameters that increase the uncertainty of the inversion problem. We have performed inversions both with and without temporal smoothing. We prefer the results of the fully independent inversion, as it is less affected by artificial constraints. It is important because if we observe a correlation of results in different time periods, we can claim that this is a real observation representing the real Earth, and not the result of artificial smoothing.

4. Verification

We are aware of the risks when interpreting temporal variations in tomographic models. In particular, study of the posterior residuals after the inversion shows that the dataset used in this study is rather noisy. Given the short source-receiver distances in this study, even strong heterogeneities hardly provide large relevant residuals. Thus, noise is a considerable component of the data in addition to signal, which explains the moderate variance reduction in some years (see Fig. 2C). The influence of random noise on the final result can be estimated using the “odd/even test” which consists in independent inversions of two data subsets separated using odd (1, 3, 5...) and even (2, 4, 6...) numbers of events. The inversion procedure is identical to the one used to derive the main results. The results of the reconstructed V_p/V_s ratio for the two subsets in different years from 2003 to 2006 are presented in the vertical section in Fig. 3 (results in other years are similar and not presented to save the space). In these images, one can immediately identify which anomalies are trustworthy and which ones are caused by noise. For example, in 2006 for the odd subset along the left (south) side of the cross section we observe low V_p/V_s , while for the even subset, the V_p/V_s ratio is high. Same discrepancies are observed in other years mostly in marginal areas. Thus, they should be ignored or interpreted with prudence. At the same time, the anomalies in the central part of the study area seem to be consistent. Note that halving of anomalies in the odd/even test lead to the resolution decrease in some parts of the models. For example, the shallow anomaly beneath Kluchevskoy in 2004 is less prominent in the odd/even tests than in the main model. All these facts should be taken into account when interpreting the inversion results.

Table 1
1D velocity distribution used as a reference model for all datasets.

Depth, km	P-velocity, km/s
–5	4.0
5	5.0
30	6.7
55	8.1
70	8.2

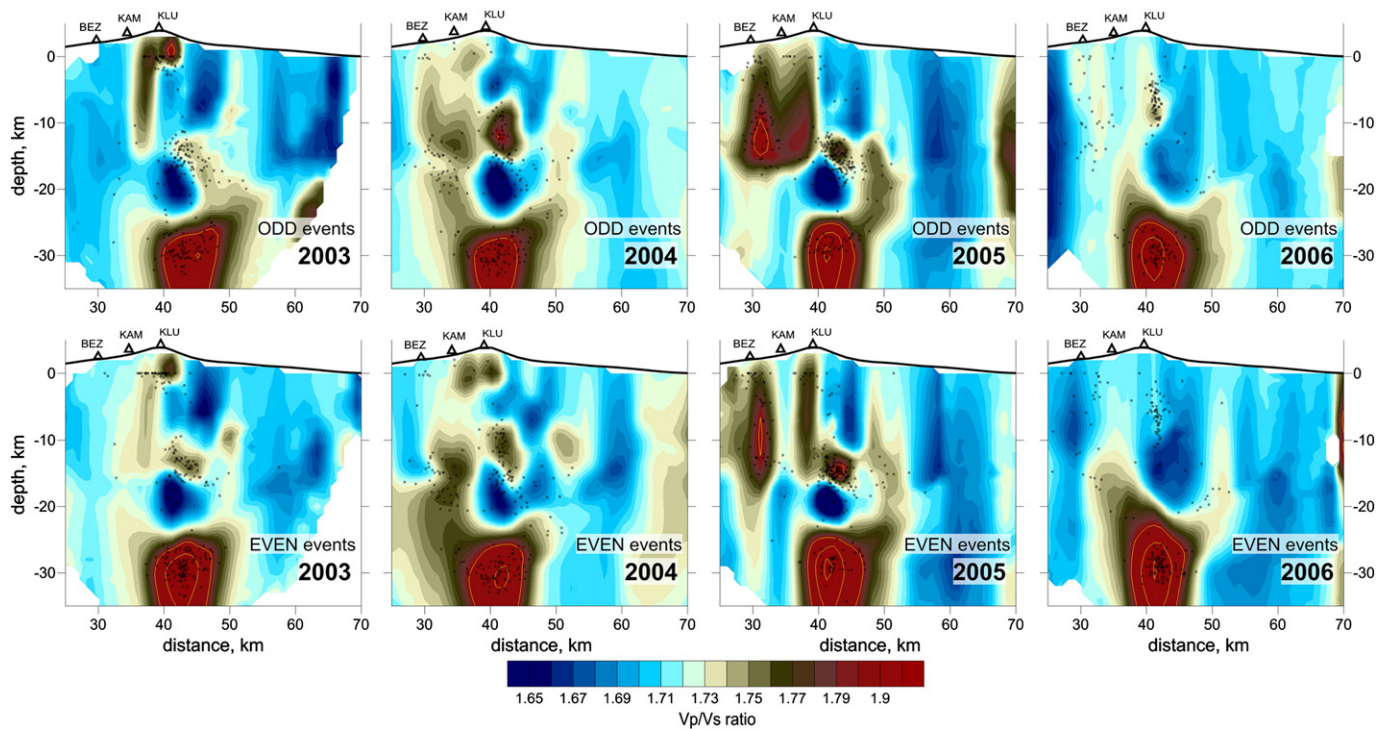


Fig. 3. Odd-even test: results of the independent inversions for two equal data subsets, each based on just half of the total input data. The resulting distributions of the V_p/V_s ratio are presented in vertical section for years 2003 to 2006. Dots depict the earthquakes within 0.5 km the profile; triangles on the surface mark the locations of volcanoes close to the profile.

It is much more difficult to estimate the effect of varying ray configurations between different time periods on the model variations. To assess this, we have performed a series of synthetic tests with realistic patterns and checkerboards. The synthetic tests were performed in a way that reproduces the procedures for real data processing, as far as possible. The travel times are computed for sources and receivers corresponding to the real observations in different years using 3D ray tracing by the bending algorithm. The travel times are then perturbed with noise with a predefined RMS for P and S data (0.1 and 0.15 s, respectively) that enables similar variance reductions for synthetic data as for observed data. The noise was produced by a random number generator with the statistical distribution corresponding to the residuals in real earthquake catalogs. After computing the synthetic travel times, we “forget” the hypocenters, origin times and the velocity distribution. The reconstruction of the synthetic model is performed in the same way as the real data processing including the estimation of the initial source location using the starting 1D model. We use the same values of free parameters (damping, smoothing, grid spacing etc.) as in the real case.

In Fig. 4 we present reconstructions of the synthetic model with realistic anomalies. The anomaly shapes were traced manually using the real data results for 2003. The upper left plot represents a cross section through the synthetic model with the P and S anomalies (in percent) and the corresponding V_p/V_s ratio. Other plots in Fig. 4 show the reconstructed distributions of V_p/V_s ratio using the data from years 2003 to 2007. The resolved patterns in the central part of the study area are similar and appear independent of the variable data sampling in different years. However, there are some minor differences, such as a small shallow pattern beneath the Kluchevskoy volcano, which is clearly seen in 2003 to 2005, but less prominent in 2006 and 2007. The reconstructed velocity distributions show that the results are somewhat dependent on the distribution of events and ray paths and are different from the original synthetic model for some years. Fig. 4 results

serve as a guide illustrating which regions of the actual model are robust (when synthetic reconstructions are similar), and which are less so (where synthetic results are different). Fortunately the majority of seismicity occurred in the deep cluster during most years, and ray configurations did not change considerably. Thus the general patterns, discussed below, are robust and represent real temporal variations of seismic parameters.

We have also performed traditional checkerboard tests for different time episodes. The alternating anomalies in the synthetic starting model (not shown) are $5 \times 5 \times 5$ km with 2 km of empty space between anomalies. The anomalies of opposite signs for P and S-models have magnitudes of 4% and –7%, respectively. These anomalies produced high contrast V_p/V_s features of similar to the real data. In Fig. A1 the results of the checkerboard reconstruction are presented in the same section as used for showing the main results. The checkerboard test results in most episodes show good vertical resolution beneath Kluchevskoy volcano and allows robust retrieval of the negative–positive–negative V_p/V_s series from 0 to 20 km depth. For the surrounding areas the resolution changes with time: in 2004, 2007 and 2008 the resolved area seems to be larger than in other years. For the deep part below 25 km depth, where we detected a prominent anomaly related to the mantle channel, this checkerboard seems to be not well resolved. Comparing the results of this test with those in Fig. 4 shows that the mantle channel can only be resolved if the anomaly is much larger than the size of the checkerboard patterns.

Note that the limited vertical resolution of our synthetic tests is partly caused by the trade-off between velocity model and source coordinates which are initially “unknown”. In this case the resolution looks poorer than in some other studies with similar observation schemes where the sources were fixed during the synthetic reconstructions. Nevertheless we claim that our way is more adequate as representing a workflow which is closer to the real data processing and therefore it display more realistic image of the resolution capacity.

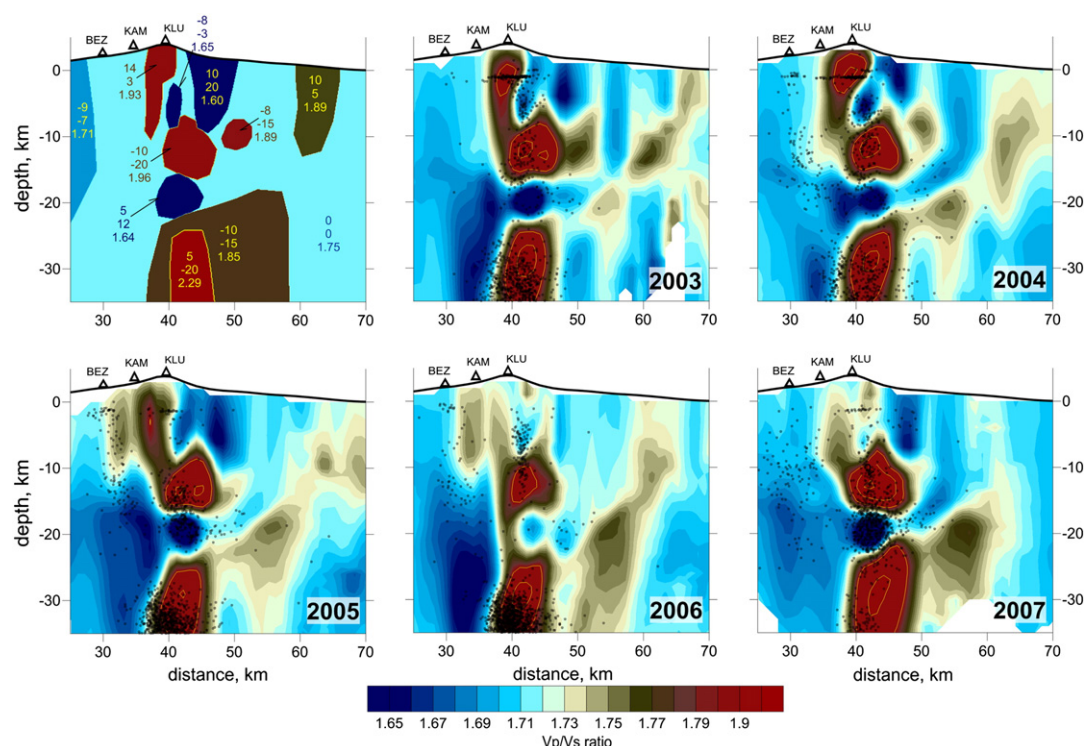


Fig. 4. Synthetic test using realistic features. The original synthetic model is shown in the upper-left plot; numbers in front of each pattern depict P- and S-anomalies, in percent, and the V_p/V_s value. Reconstructions of the V_p/V_s ratio for 2003 to 2006 are presented in the vertical cross-section. Dots depict the earthquakes within 0.5 km of the profile.

Another important conclusion from tests is that computing V_p/V_s ratio by subdivision of independently derived P- and S-velocities appears to be adequate. One may expect that some uncertainties in P- and S-velocity fields due to uneven ray sampling are amplified when computing their ratio. Actually, these tests show that this scenario does not cause apparent instability, and the resolved V_p/V_s ratio looks consistent with the input model.

5. Variations in the seismic structure through time

The travel time misfit is an important argument for the existence of strong temporal variations in structure. These parameters reflect how well the derived velocity model satisfies the observed data. As discussed in Section 3, the variance is reduced by just 15% for the simultaneous inversion of all data—a very low reduction for tomographic inversion. The full dataset cannot be fit by a single model. In Fig. 2C and D we present the variance reductions and RMS travel time residuals for forty inversions of overlapping subsets corresponding to yearly windows with three months of time steps in a period from 1999.01.01 to 2009.12.31. When inversions were performed in one-year windows, the variance reductions were generally higher than for the case of the simultaneous inversion. Note that in the case of the entire dataset, we selected only the best events with a maximum number of picks, while for the yearly subsets, we used more data of poorer quality. While this would normally ensure lower noise and higher variance reduction, the fact that we observe a larger variance reduction means that there are considerable time variations in velocity.

The variance reduction presented in Fig. 2C is variable in time. Small reductions before 2002 may be due to the low number of stations and poorer data quality. The highest variance reduction was obtained for the time periods 2003 and 2005–2006 when the volcano was most active. This can be explained by the presence of higher magnitude earthquakes which are picked with higher accuracy. The travel times

were best fit in 2006 (Fig. 2D) corresponding to the period of post-eruptive relaxation.

Yearly inversion results from 2001 to 2008 for P- and S-velocity anomalies and V_p/V_s ratio are presented in Figs. 5 to 7 along a vertical section that passes through the active Kluchevskoy and Bezmyanny volcanoes and the dormant Zimina and Kamen volcanoes. We also present V_p and V_s anomalies and V_p/V_s ratio for yearly time windows in horizontal sections at 12 km and 30 km depth in the auxiliary materials (Figs. A2 and A3). The distributions of V_p/V_s ratio in the same vertical section as in Figs. 5–7 for the entire series of 40 overlapping time windows (one year with the step of three months) are presented in auxiliary materials, Fig. A4.

We focus our interpretations on V_p/V_s values, which are most sensitive to the distribution of fluids and melts (Fig. 7). The final distribution of earthquakes in each data subset are presented in the same sections.

The deepest anomaly, located in the center of the Kluchevskoy group below 25 km depth, is robustly resolved in all time periods and is seen in all horizontal and vertical sections representing the real data results (Figs. 5 to 7 and A2 to A4), except for the time windows prior to the year 2000, when the data volume and quality was insufficient. Within this anomaly, we observe positive P- and very strong negative S-velocity anomalies, leading to unusually high V_p/V_s values, up to 2.2. In the upper part of this anomaly, there are dense clusters of seismicity that release most of the seismic energy in the study area.

In the crust, we observe several important features that evolve coherently with the main periods of volcanic activity. From 2001 to 2004, in Fig. 7 we see two weakly variable anomalies of high V_p/V_s values located at 8–13 km depth and 0 km depth beneath Kluchevskoy. These features probably represent two intermediate magma reservoirs that accumulate melts and fluids prior to an eruption.

In 2005, the velocity model changes abruptly, expressed by a considerable increase in the average V_p/V_s value. The highest V_p/V_s is observed beneath Bezmyanny, where a strong eruption occurred in 2005. This feature appears as a direct linking the volcano with the mantle anomaly.

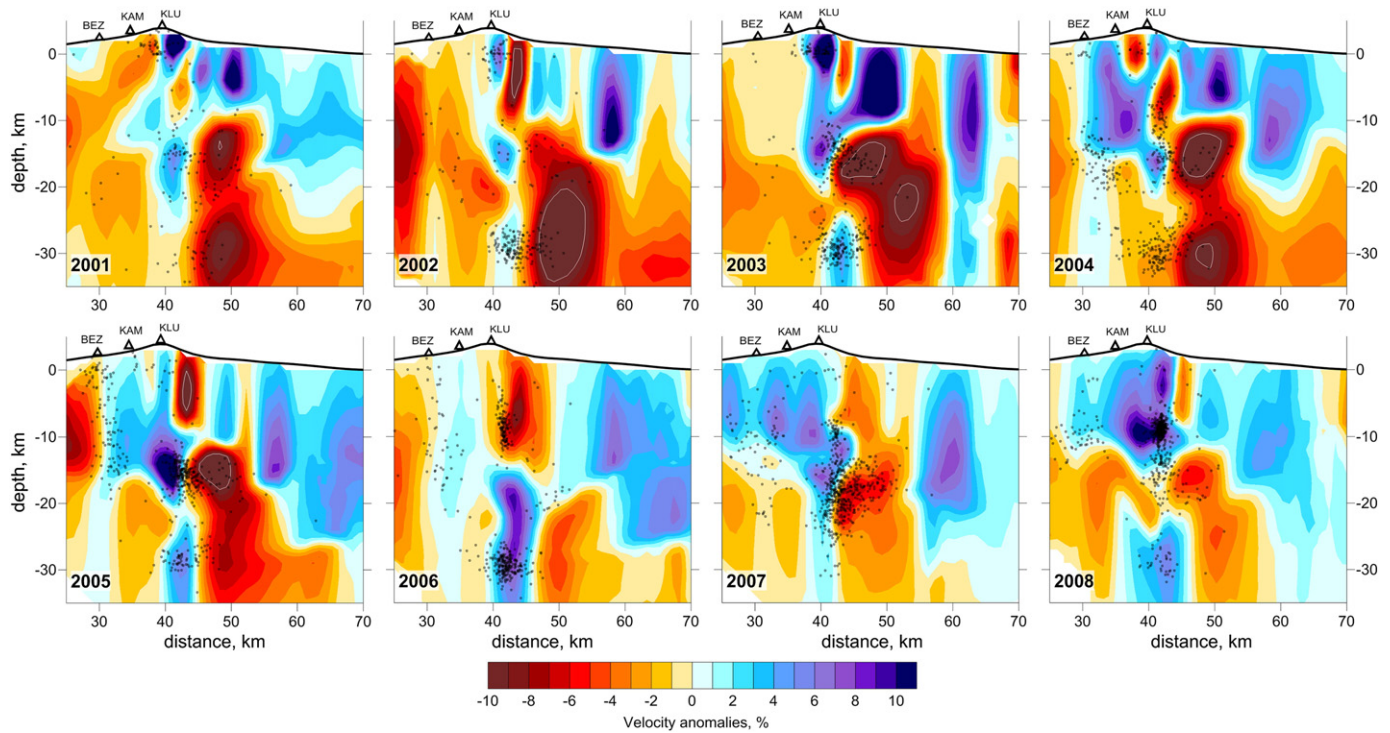


Fig. 5. P-velocity anomalies in vertical cross-section for 2001 to 2008. The location of the profile is shown in Fig. 1B. In areas of low V_p , white lines show contours of $dV_p = -15\%$. Dots show earthquakes within 0.5 km from the profile, and triangles mark the locations of volcanoes.

Beneath Kluchevskoy, where a nearly simultaneous eruption took place, the anomaly observed in 2005 and prior disappeared.

In 2006 and 2007, no anomalies in the middle and upper crust are observed; only the deep high V_p/V_s anomaly is clearly detected. In 2008, a high V_p/V_s anomaly appears again at depths between 8 and 15 km.

6. Discussion

The most striking feature of the model is an anomaly with very high V_p/V_s ratio located below 25 km depth that remains unchanged over large periods of time. Higher P-velocities, which are sensitive to

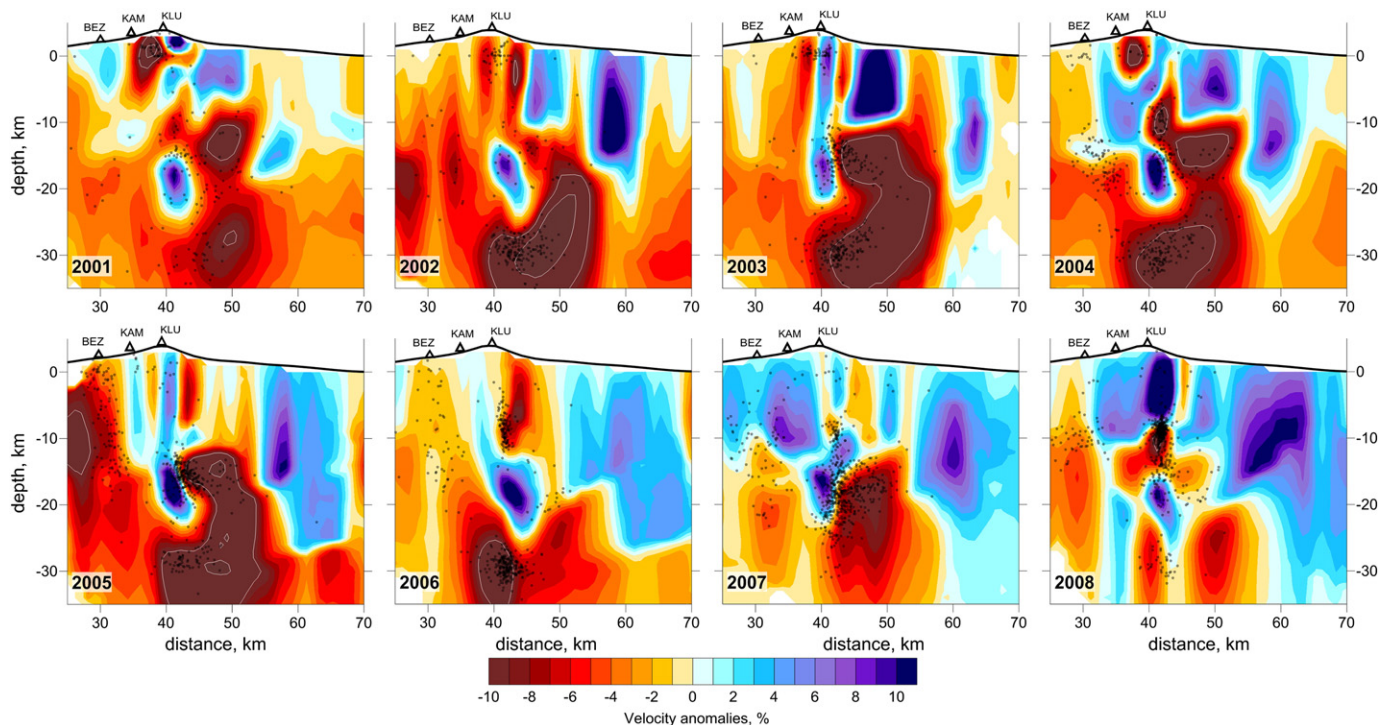


Fig. 6. S-velocity anomalies in vertical cross-section for 2001 to 2008. The location of the profile is shown in Fig. 1B. In areas of low V_s , white lines show contours of $dV_s = -15\%$ and -20% . Dots show earthquakes within 0.5 km of the profile, and triangles mark the locations of volcanoes.

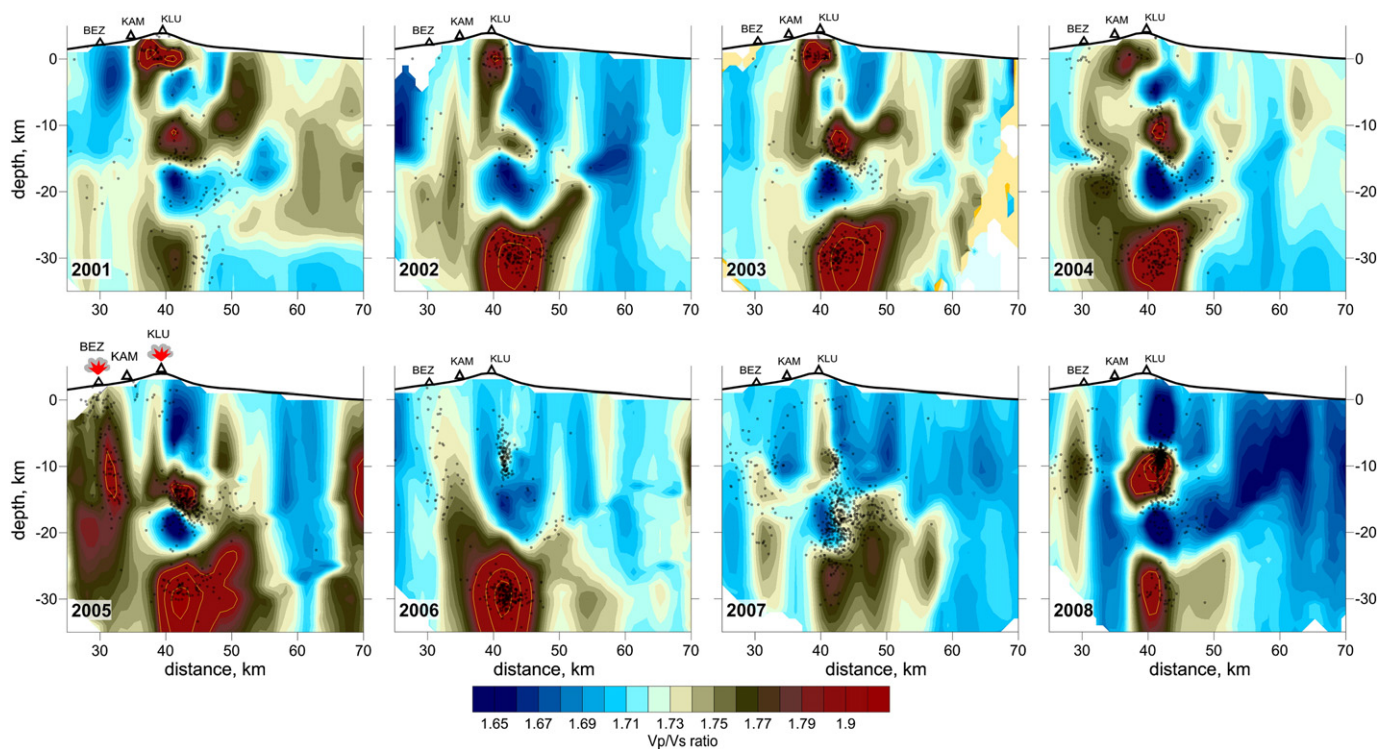


Fig. 7. Cross-sections of V_p/V_s for 2001 to 2008. The location of the profile is shown in Fig. 1B. In areas of high V_p/V_s , yellow lines show contours of $V_p/V_s = 2.0, 2.1$ and 2.2 . Dots show earthquakes within 0.5 km of the profile, and triangles mark the locations of volcanoes. Eruptions of Kluchevskoy and Bezmianny volcanoes in 2005 are highlighted. (For interpretation of the references to color in this figure legend, the reader is referred to the web version of this article.)

composition, coexist here with very low S-velocities, reflecting the existence of melts and fluids. This observation can be explained by the presence of a channel that brings fluid and melt rich materials from the mantle. This channel probably starts on the upper surface of the slab as proposed by Dobretsov (2010). Such flows, or hot fingers, appear to be a typical feature sourcing volcanoes in subduction zones and are seen clearly in high resolution tomographic images (e.g. Tamura et al., 2002). Previously the existence of hot fingers was predicted by Dobretsov and Kiryashkin (1997) based on results of modeling, petrological, geochemical and geophysical data.

In contrast to the lower part of the model, the structure in the middle and upper crust appears to be strongly variable in time. In 2001 to 2004 we observe two anomalies of high V_p/V_s ratio in the mid-crust and just below Kluchevskoy. In 2005, we detect an abrupt change in seismic parameters coinciding with the almost simultaneous eruptions of Kluchevskoy and Bezmianny volcanoes. In 2006 to 2007, generally low V_p/V_s ratio without any considerable heterogeneity is observed in the crust. In 2008, an anomaly of high V_p/V_s ratio appears again in the mid-crust.

From a physical and mechanical point of view, it is not plausible to explain these fast changes with mechanical transport of large masses or strong variations of the temperature in the crust. We propose that the observed changes of seismic parameters are related to variations of the stress and deformation fields and fast fluid transport through the rocks of the crust. To explain the features recovered in the 4D seismic model, we propose the qualitative scenario illustrated in Fig. 8.

We believe that major processes in the crust beneath the Kluchevskoy group of volcanoes originate in a mantle channel observed in the lowermost part of the model in all time windows. Mechanically, thermally or chemically, the mantle channel affects the lower crust and causes excessive pressure and stresses. This leads to the opening of cracks and the transportation of fluids and melts upward. When

they reach an intermediate level (10–12 km depth) these fluids lower the melting temperature of overheated rocks and trigger the creation of magma sources (e.g., Kohn, 2000; Giordano et al., 2004). At the same time, decompression may lead to the formation of gas bubbles that increase the pressure around the intermediate magma reservoirs (see, for example, Lensky et al., 2004). In turn, this causes the origin of new fractures and the further activation of fluid transport through the crust. This avalanche-type positive feedback ultimately ends in eruption (Fig. 8B).

It is interesting that we observe a strong increase of V_p/V_s ratio beneath Bezmianny volcano at the time of the Kluchevskoy eruption in 2005. We can propose that the feeding of Kluchevskoy volcano occurs through a complex system of intermediate magma reservoirs in the crust, while Bezmianny volcano appears to be connected with the mantle source through a direct short-lived channel. These structures may explain the different composition and eruption style of these volcanoes. This concept is generally consistent with findings of a multidisciplinary study of deep sources of magmatism beneath the Kluchevskoy group by Fedotov et al. (2010).

After a relatively short phase of activity in 2005, we observe a relaxation period in 2006 and 2007, when intermediate magma sources are not seen in the tomography results. However, it would be incorrect to claim that the intermediate chambers disappeared during this period. The observed intensive seismicity at corresponding depths suggests that the chambers continue to be active. We propose that after finishing the eruptions (Fig. 8C), stresses in the crust are released, and cracks are predominantly closed. A deficit of fluids at this stage decreases the melt content (e.g., Giordano et al., 2004), and magma reservoirs in the crust become less prominent. This post-eruptive relaxation stage lasts for two years. In 2008, an intermediate depth anomaly of high V_p/V_s ratio surrounded by clusters of seismicity reappears at the same location as in 2001–2004. This probably indicates another phase of periodic

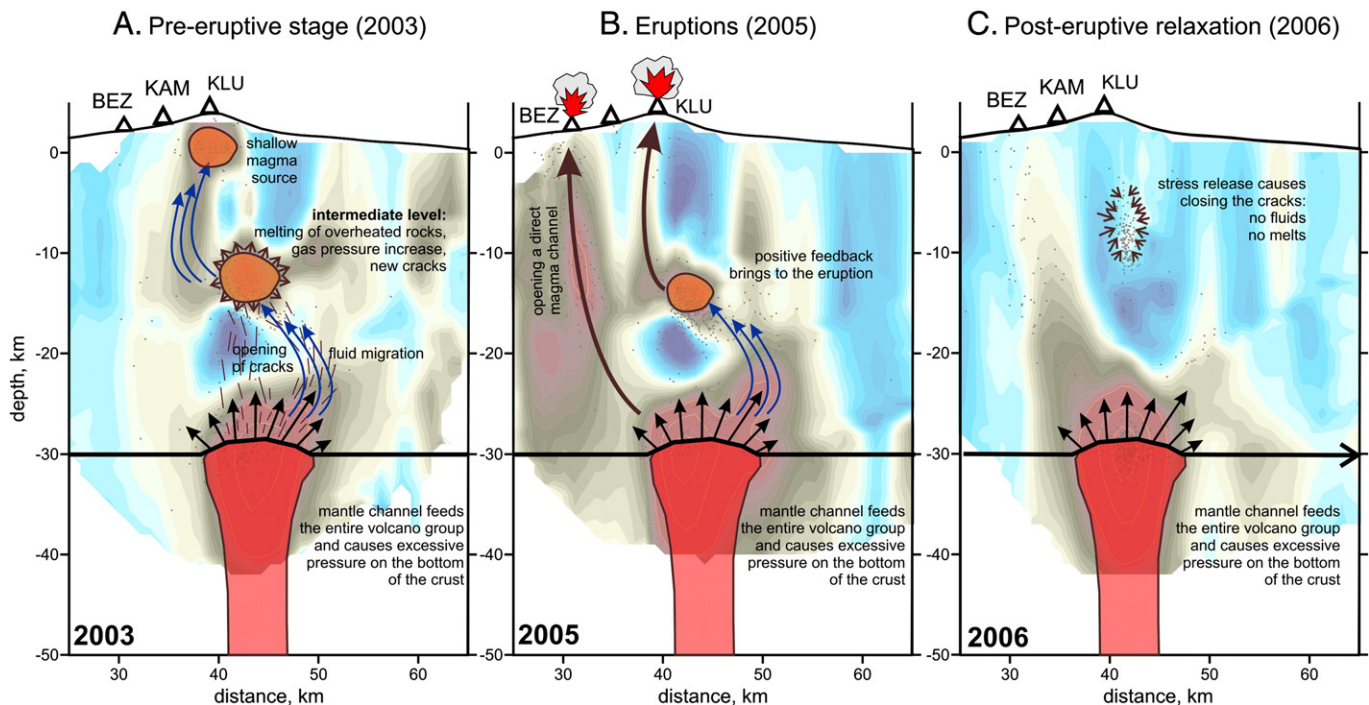


Fig. 8. Stages of the eruption cycle in the Kluchevskoy group of volcanoes based on 4D tomography. The background is V_p/V_s distribution in vertical cross-section corresponding to 2003, 2005 and 2006. A) In the pre-eruptive stage excessive pressure produced by the mantle channel causes stresses and crack formation in the crust. Fluid migration to mid-crust levels causes melting of overheated rocks and gas bubble growth due to decompression. This leads to additional stresses and new fractures. B) Positive feedback between fluid migration, melting and crack formation result in the eruption of Kluchevskoy volcano in the beginning of 2005. At this stage we observe a short-lived opening of a channel directly from the mantle that feeds the Bezmianny eruption in approximately same time. C) After the eruptions, the stresses are released and the cracks are closed. A deficit of fluids triggers the solidification of magma at intermediate depths.

activation and partial melting within the magma chamber. A shallow chamber beneath Kluchevskoy volcano was not yet visible in the latest images. It should be noted that shortly after this study period Kluchevskoy began a protracted eruption sequence that lasted through the end of 2010 (KVERT, 2001–2010). In addition, Bezmianny experienced its most explosive recent eruptions at the end of 2009 and in early 2010 (West, this issue). It is quite likely that the new mid-crustal anomaly that appeared in 2008 is the magma reservoir which sourced the eruptions of 2009–2010.

7. Conclusions

In this study we present time dependent distributions of seismic parameters beneath the Kluchevskoy group of volcanoes for the period 2001 to 2008 based on repeated tomographic inversions in yearly time windows. The robustness of the time variations is supported by synthetic tests with reconstructions of a common model using data selected from the moving time window.

One of the most important findings is a feature below 25 km depth with extremely high V_p/V_s ratio reaching 2.2. This feature with higher P- and very low S-velocities is probably an image of the top part of a mantle channel which brings deep mantle material with high fluid and melt content. This mantle “finger” appears to be directly or indirectly responsible for all volcanic activity in the Kluchevskoy group.

The significant variations in seismic parameters in the crust seem to have a direct link with the eruptive activity of the volcanoes. The distribution of seismic velocities and V_p/V_s values allows the magma sources beneath the volcanoes to be tracked in time and allows us to surmise their role in volcanic activity. The major changes are observed in 2005 when eruptions of Bezmianny and Kluchevskoy occurred almost in the same time. It is seen that Kluchevskoy is fed through a complex system of intermediate reservoirs in the crust, while Bezmianny

seems to be linked with the mantle “finger” through a short-lived direct channel.

Beyond the mechanics of the Kluchevskoy group, this study is important because it shows that seismic features frequently inferred to represent magma storage zones are dynamic in time. Prominent features appear and disappear on the scale of years. We propose that sponge-like magma reservoirs filled with melt can be caused by the rapid migration of fluids through overheated crustal rocks. In turn, the fluid migration is triggered by variations in the stress field and quickly facilitated by the highly fractured nature of volcanic crust. Following eruptions, the fluid deficit and the relaxation of fracture pathways may decrease the melt content leading to the temporary disappearance of seismic anomalies in the V_p/V_s images. A similar concept of a sponge-like network of interconnected fractures and melt bodies beneath volcanoes is envisaged by Lu and Dzurisin (2010) based on surface deformation observations.

It is possible that continued tomographic monitoring will allow the prediction of catastrophic eruptions in the future, by observing precursors in the time-dependent seismic structure. This 4D approach should be applied in other volcanic areas of the world to check if the features found in this study are observed elsewhere.

Acknowledgments

This study is supported by the multidisciplinary project SB-DVO RAN #42, Integration Project of SB RAS #20 and ONZ-7.3. We are grateful to two anonymous reviewers for thorough analysis of the manuscript and constructive comments that greatly improved the paper. We express special thanks to Michael West who made considerable work on editing the manuscript and including some very important points on the scientific content into the paper.

Appendix A. Auxiliary materials

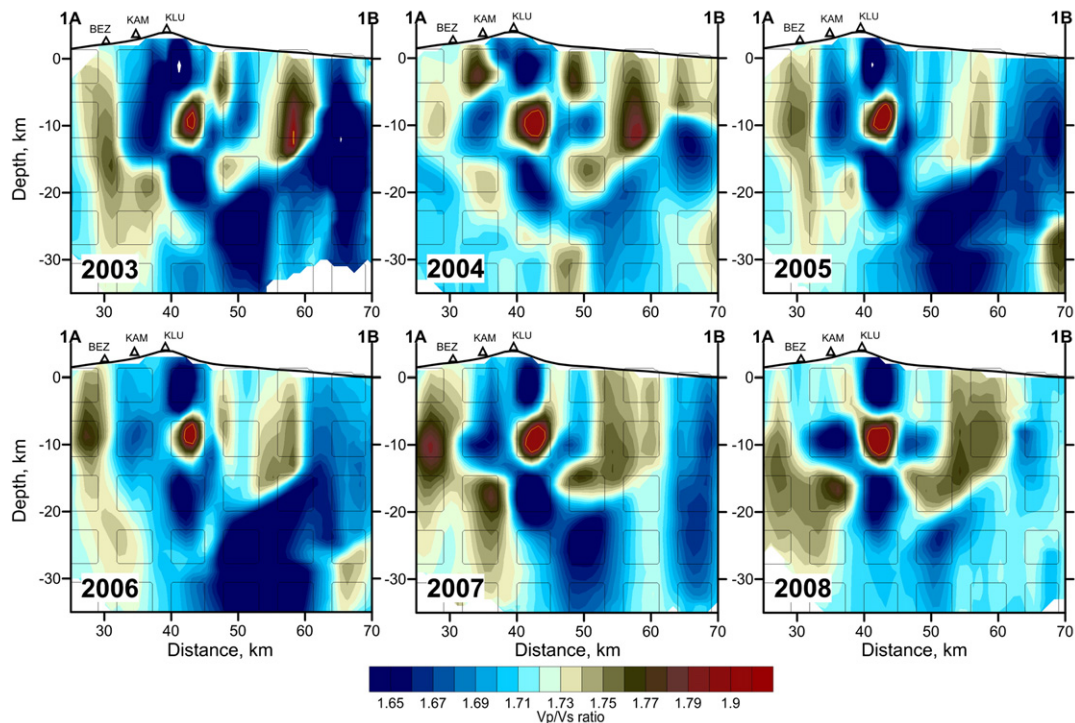
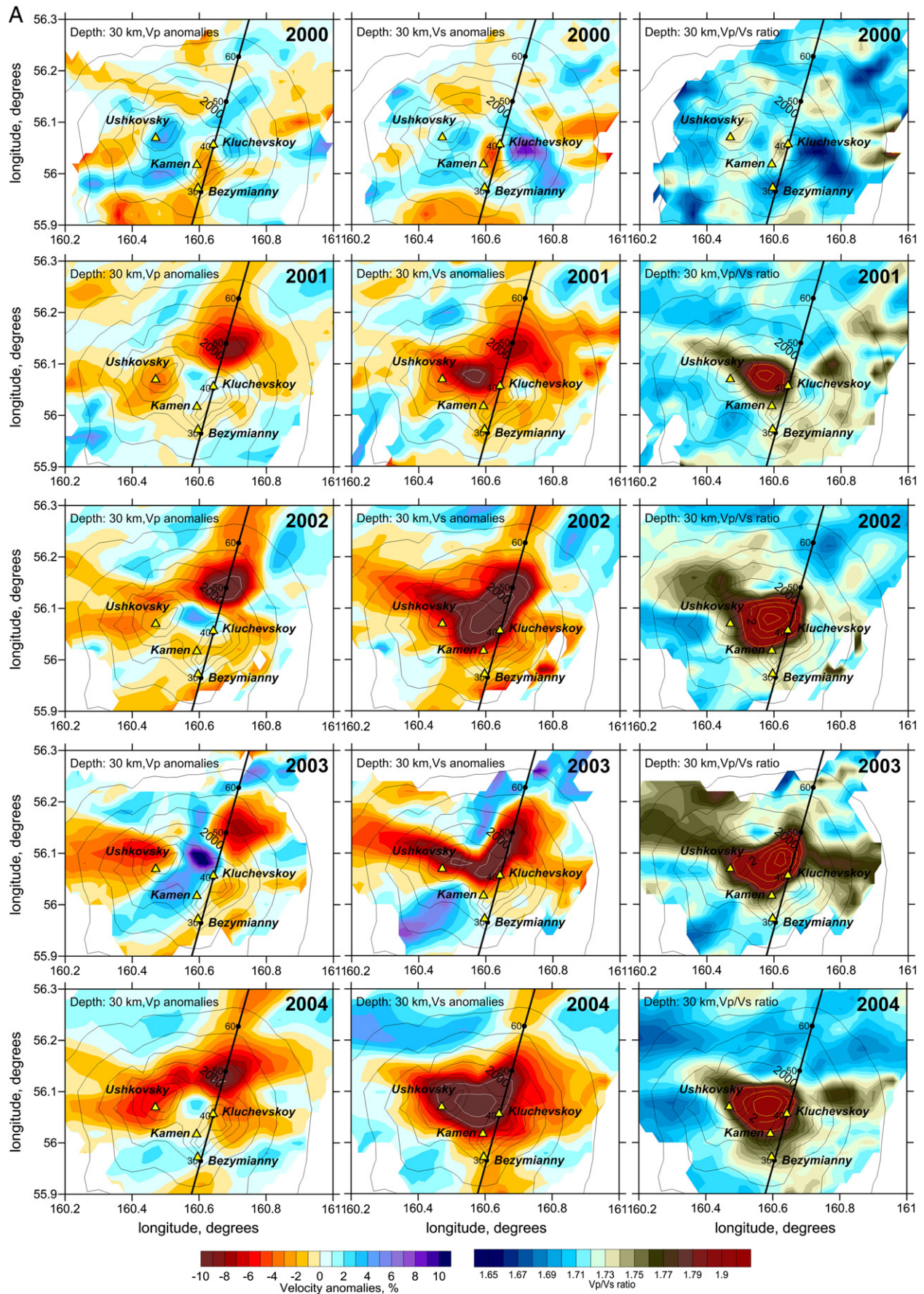


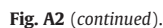
Fig. A1. Results of the checkerboard test. The true anomalies are marked with thin lines. The strong variations in V_p/V_s ratio in the synthetic model are due to anticorrelating P- and S-anomalies having amplitudes of -4 and 7% , respectively. The distributions of the resolved V_p/V_s ratio are presented in the vertical section, same as in Fig. 7.

References

- Dobretsov, N.L., 2010. Distinctive petrological, geochemical and geodynamic features of subduction-related magmatism. *Petrology* 18 (N1), 84–106.
- Dobretsov, N.L., Kirdyashkin, A.G., 1997. Modeling of subduction processes. *Russian Geology and Geophysics* 37 (5), 846–857.
- Fedotov, S.A., Zharinov, N.A., Gontovaya, L.I., 2010. The magmatic system of the Klyuchevskaya Group of volcanoes inferred from data on its eruptions, earthquakes, deformation and deep structure. *Volcanology and Seismology* 1, 3–35.
- Giordano, D., Romano, C., Poe, B., Dingwell, D.B., Behrens, H., 2004. The combined effects of water and fluorine on the viscosity of silicic magmas. *Geochimica et Cosmochimica Acta* 68, 5159–5168.
- Gorbatov, A., Dominguez, J., Suarez, G., Kostoglodov, V., Zhao, D., Gordeev, E., 1999. Tomographic imaging of the P-wave velocity structure beneath the Kamchatka peninsula. *Geophysical Journal International* 137, 269–279.
- Gorbatov, A., Fukao, Y., Widiyantoro, S., Gordeev, E., 2001. Seismic evidence for a mantle plume oceanwards of the Kamchatka–Aleutian trench junction. *Geophysical Journal International* 146 (2), 282–288.
- Gorshkov, G.S., Bogoyavlenskaya, G.E., 1965. The Bezmianny Volcano and peculiarity of the last eruption (1955–1956). Nauka, Moscow, pp.165.
- Graeber, F.M., Asch, G., 1999. Three-dimensional models of P wave velocity and P-to-S velocity ratio in the southern central Andes by simultaneous inversion of local earthquake data. *Journal of Geophysical Research* 104, 20,237–20,256.
- Hoffmann-Rothe, A., Ibs-von Seht, M., Knies, R., Klinge, K., Reichert, C., Purbawinata, M.A., Patria, C., 2006. Monitoring Anak Krakatau Volcano in Indonesia. *Eos, Transactions, American Geophysical Union* 87 (51), 581 (585–58).
- Ivanov, V.V., 2008. Current cycle of the Klyuchevskoy volcano activity in 1995–2008 based on seismological, photo, video and visual data. *Proceedings of Conference, Petropavlovsk-Kamchatsky*, 27–29 March, pp. 100–109.
- Julian, B., Foulger, G., 2010. Time-dependent seismic tomography. *Geophysical Journal International* 182, 1327–1338.
- Khrenov, A.P., Antipin, V.S., Chuvashova, L.A., Smirnova, E.V., 1989. Petrochemical and geochemical peculiarity of basalts of the Klyuchevskoy volcano. *Volcanology and Seismology* 3, 3–15.
- Khubunaya, S., Gontovaya, L., Sobolev, A., Nizkov, I., 2007. Magmatic sources beneath the Klyuchevskoy volcano group (Kamchatka). *Volcanology and Seismology* 2, 22–42.
- Kohn, S.C., 2000. The dissolution mechanisms of water in silicate melts: a synthesis of recent data. *Mineralogical Magazine* 64, 389–408.
- Koulakov, I., 2009. LOTOS code for local earthquake tomographic inversion. *Benchmarks for testing tomographic algorithms. Bulletin of the Seismological Society of America* 99 (1), 194–214.
- Koulakov, I.Yu., Dobretsov, N.L., Bushenkova, N.A., Yakovlev, A.V., 2011a. Slab shape in subduction zones beneath the Kurile–Kamchatka and Aleutian arcs based on regional tomography results. *Russian Geology and Geophysics* 52, 650–667.
- Koulakov, I., Gordeev, E.I., Dobretsov, N.L., Vernikovskiy, V.A., Senyukov, S., Jakovlev, A., 2011b. Feeding volcanoes of the Klyuchevskoy group from the results of local earthquake tomography. *Geophysical Research Letters* 38, L09305.
- KVERT, 2001–2010. Kamchatkan and Northern Kuriles Volcanic Activity Daily Information Releases. <http://www.kscnet.ru/ivs/kvert/updates.php> (Petropavlovsk-Kamchatsky. Last accessed May 10, 2012).
- Laverov, N.P. (Ed.), 2005. *Modern and Holocene Volcanism in Russia*. Nauka, Moscow, pp. 604.
- Lees, J.M., Van Decar, J., Gordeev, E., Ozerov, A., Brandon, M., Park, J., Levin, V., 2007a. Three Dimensional Images of the Kamchatka-Pacific Plate Cusp. In: Eichelberger, J., Gordeev, E., Kasahara, M., Izbekov, P., Lees, J.M. (Eds.), *Volcanism and Subduction: The Kamchatka Region*. American Geophysical Union, Washington, D.C., pp. 65–75.
- Lees, J.M., Symons, N., Chubarova, O., Gorelich, V., Ozerov, A., 2007b. Tomographic Images of Klyuchevskoi Volcano P-wave Velocity. In: Eichelberger, J., Gordeev, E., Kasahara, M., Izbekov, P., Lees, J.M. (Eds.), *Volcanism and Subduction: The Kamchatka Region*. American Geophysical Union, Washington, D.C., pp. 293–302.
- Lensky, N., Lyakhovskiy, V., Navon, O., 2004. Bubble growth during decompression of magma: experimental and theoretical investigation. *Journal of Volcanology and Geothermal Research* 129, 7–22.
- Levin, V., Shapiro, N., Park, J., Ritzwoller, M., 2002. Seismic evidence for catastrophic slab loss beneath Kamchatka. *Nature* 418, 763–767.
- Lu, Z., Dzurisin, D., 2010. Ground surface deformation patterns, magma supply, and magma storage at Okmok volcano, Alaska, from InSAR analysis: 2. Coeruptive deflation, July–August 2008. *Journal of Geophysical Research* 115, B00B03. <http://dx.doi.org/10.1029/2009JB006970>.
- Nikulin, A., Levin, V., Shuler, A., West, M.E., 2010. Anomalous seismic structure beneath the Klyuchevskoy Group, Kamchatka. *Geophysical Research Letters* 37. <http://dx.doi.org/10.1016/j.jeps.2011.12.039>.

Fig. A2. The distribution of P- and S-anomalies and V_p/V_s ratio at 30 km depth corresponding to yearly time windows from 2000 to 2009. Line mark the profile for which the main results are presented. Triangles depict the active volcanoes. Contour lines show the topography.





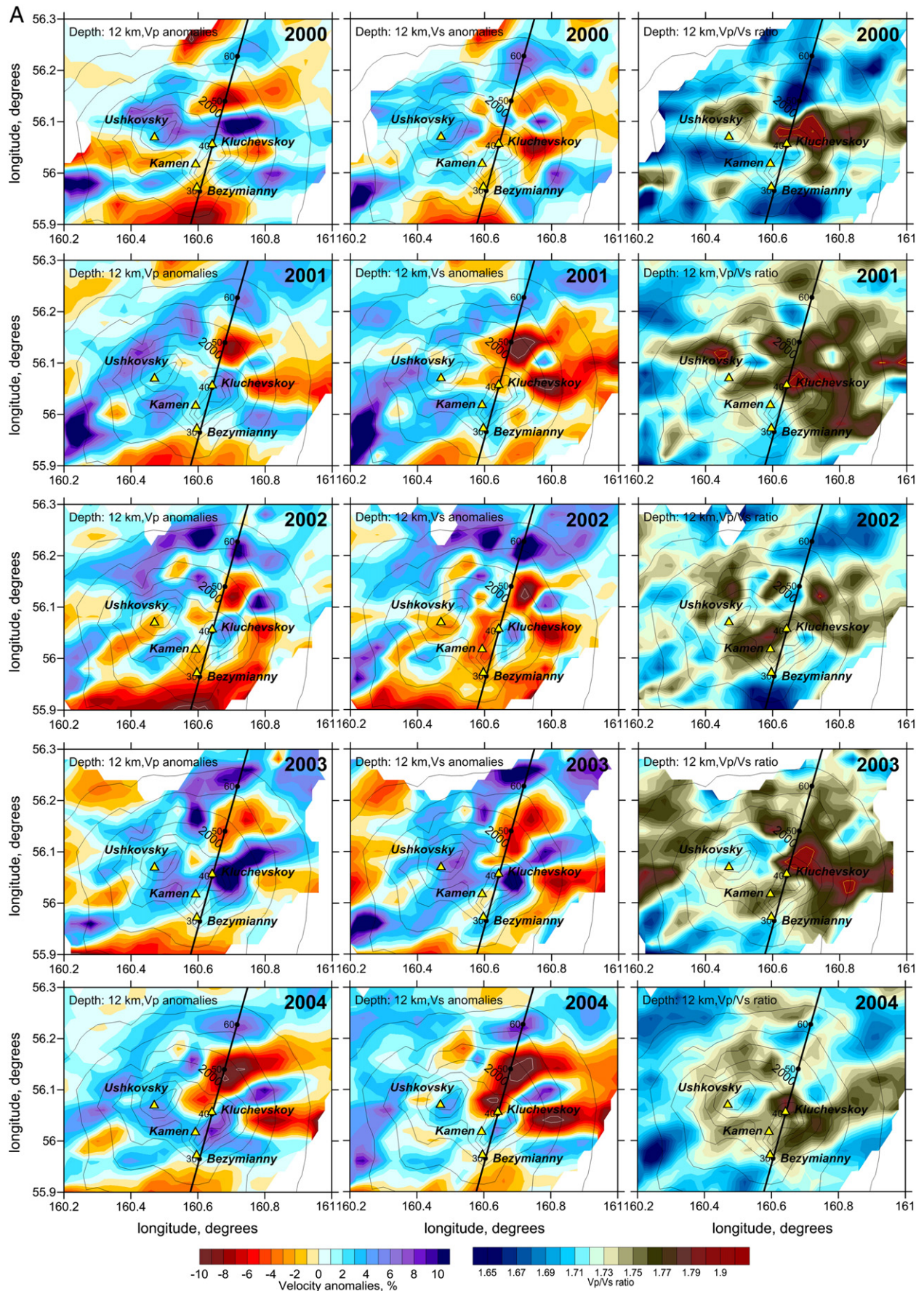
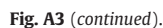


Fig. A3. The distribution of P- and S-anomalies and V_p/V_s ratio at 12 km depth corresponding to yearly time windows from 2000 to 2009. Line mark the profile for which the main results are presented. Triangles depict the active volcanoes. Contour lines show the topography.



Nikulin, A., Levin, V., Carr, M., Herzberg, C., West, M.E., 2012. Evidence for two upper mantle sources driving volcanism in Central Kamchatka. *Earth and Planetary Science Letters* 321–322, 14–19. <http://dx.doi.org/10.1029/2010GL043904>.

Nizkous, I.V., Sanina, I.A., Kissling, E., Gontovaya, L.L., 2006. Velocity Properties of the Lithosphere in the Ocean–Continent Transition Zone in the Kamchatka Region from Seismic Tomography Data. *Izvestiya, Physics of the Solid Earth* 42 (4), 286–296.

Nizkous, I., Kissling, E., Sanina, I., Gontovaya, L., Levina, V., 2007. Correlation of Kamchatka Lithosphere Velocity Anomalies With Subduction Processes. *Volcanism and Subduction: The Kamchatka Region Geophysical Monograph Series*, 172, pp. 97–106 (Copyright 2007 by the American Geophysical Union. 10/1029/172GM09, 369 pp.).

Ozerov, A.Y., Ariskin, A.A., Kyle, P., Bogoyavlenskaya, G.E., Karpenko, S.F., 1997. A petrological–geochemical model for genetic relationships between basaltic and

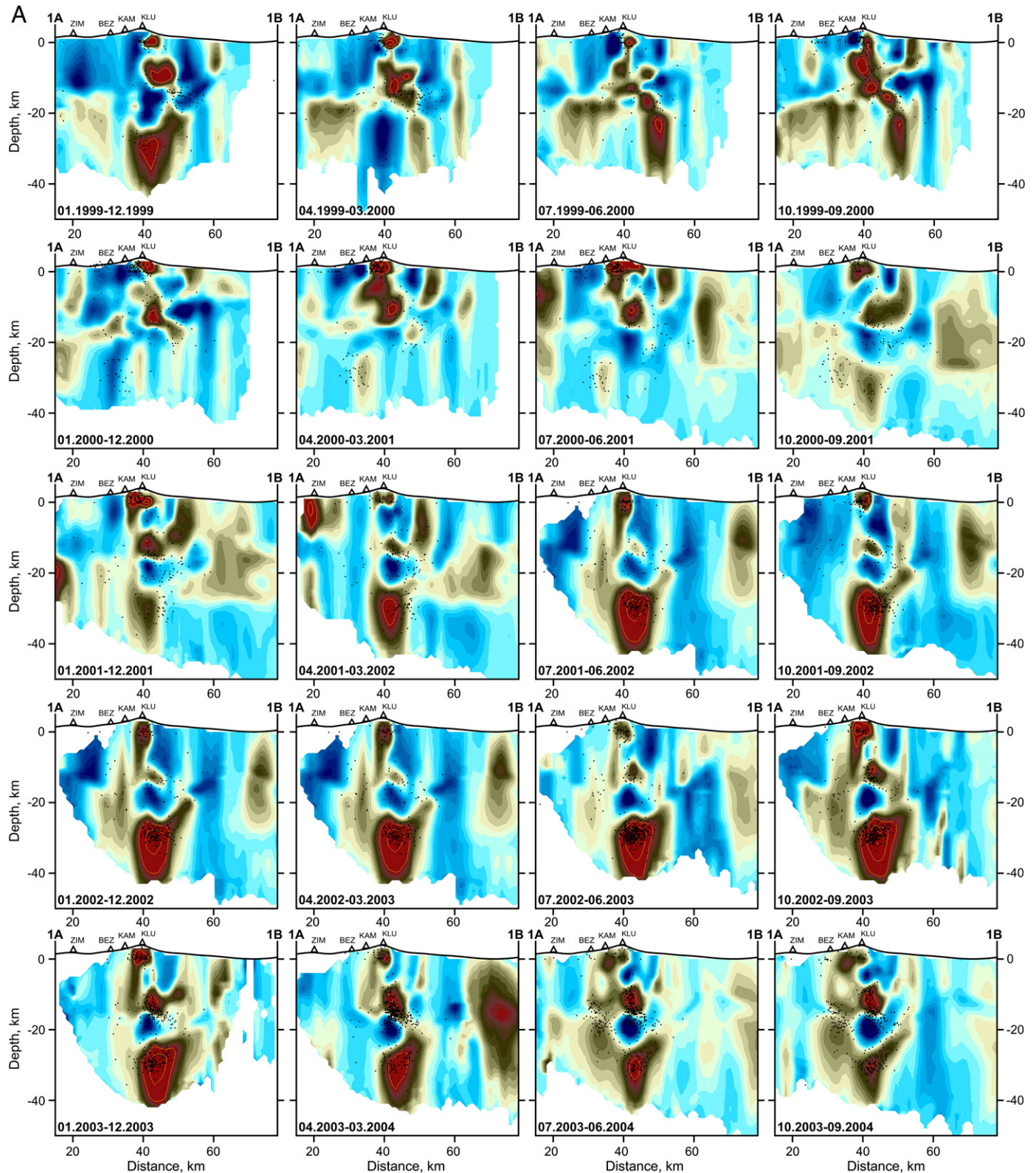


Fig. A4. Distributions of V_p/V_s ratio on the cross-section for the overlapping yearly windows with three-month steps. The location of the profile is shown in Fig. 1B. In areas of high V_p/V_s , yellow lines show contours of $V_p/V_s = 2.0$, 2.1 and 2.2. Dots show earthquakes within 0.5 km of the profile, and triangles mark the locations of volcanoes near the profile. (For interpretation of the references to color in this figure legend, the reader is referred to the web version of this article.)

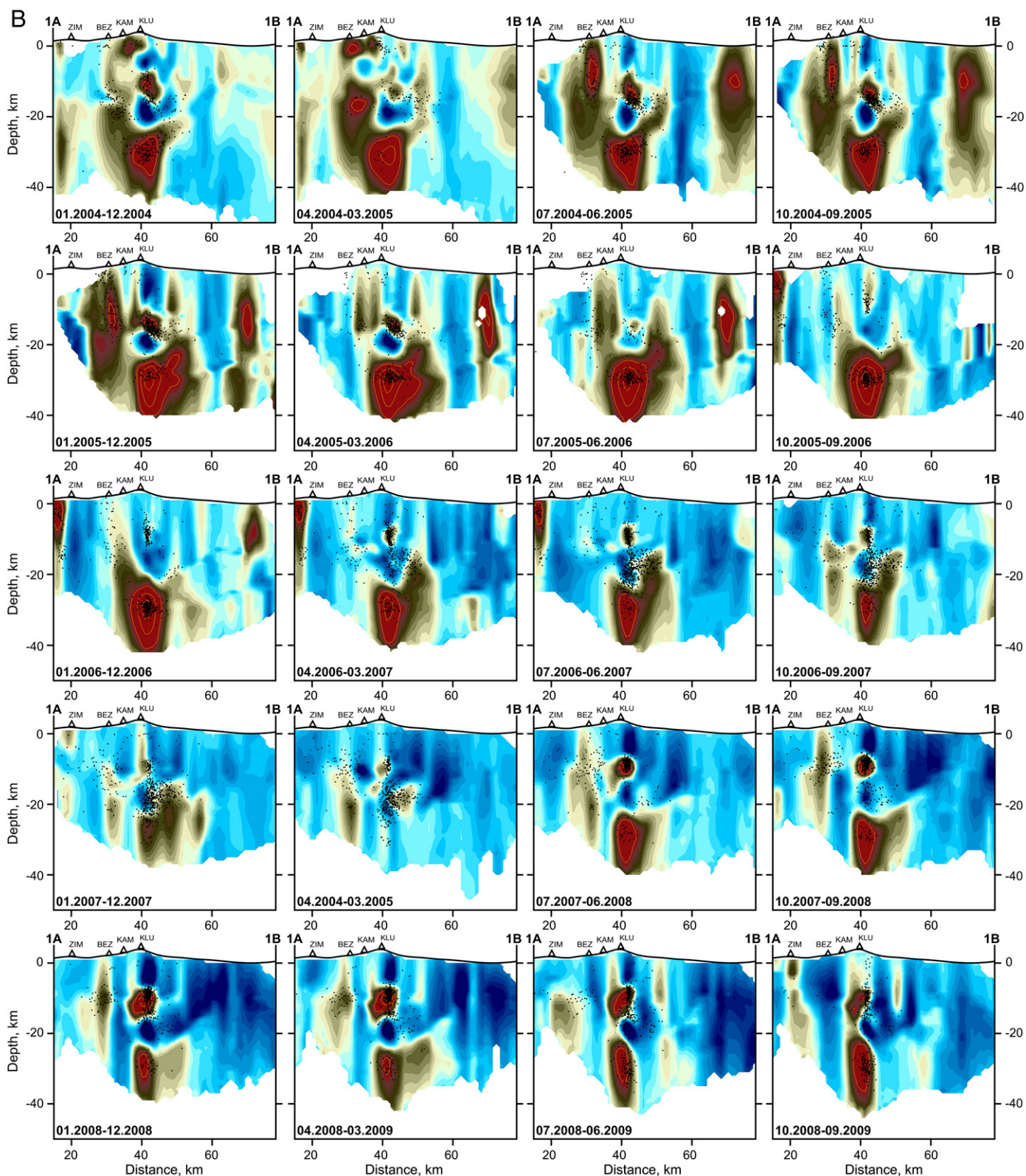


Fig. A4 (continued).

- andesitic magmatism of Klyuchevskoi and Bezmyanni volcanoes, Kamchatka. *Petrology* 5, 550–569.
- Ozerov, A.Yu., Firstov, P.P., Gavrilov, V.A., 2007. Periodicities in the Dynamics of Eruptions of Klyuchevskoi Volcano, Kamchatka. *Volcanism and Subduction: The Kamchatka Region: Geophysical Monograph Series*, vol. 172, pp. 283–291.
- Paige, C.C., Saunders, M.A., 1982. LSQR: an algorithm for sparse linear equations and sparse least squares. *ACM Transactions on Mathematical Software* 8, 43–71.

- Patanè, D., Barberi, G., Cocina, O., De Gori, P., Chiarabba, C., 2006. Time-resolved seismic tomography detects magma intrusions at Mount Etna. *Science* 313 (5788), 821–823.
- Savage, M., Wessel, A., Hurst, T., Teanby, N., 2010a. Automatic shear wave splitting and applications to time varying anisotropy at Mt. Ruapehu volcano, New Zealand. *Journal of Geophysical Research* 115, B12321.
- Savage, M.K., Ohminato, T., Aoki, Y., Tsuji, H., Greve, S., 2010b. Stress magnitude and its temporal variation at Mt. Asama Volcano, Japan, from seismic anisotropy and GPS.

- Earth and Planetary Science Letters 290 (3–4). <http://dx.doi.org/10.1016/j.epsl.2009.12.037>.
- Senyukov, S.L., Droznina, S.Ya., Nuzhdina, I.N., Garbuzova, V.T., Kozhenkova, T.Yu., 2009. Studies in the activity of Klyuchevskoi volcano by remote sensing techniques between January 1, 2001 and July 31, 2005. *Volcanology and Seismology* 3, 1–10.
- Slavina, L.B., Garagi, I.A., Gorelchik, V.I., Ivanov, B.V., Belyankin, B.A., 2001. Velocity structure and stress-deformation state of the crust in the area of the Kluchevskoy volcano group in Kamchatka. *Volcanology and Seismology* 1, 49–59.
- Tamura, Y., Tatsumi, Y., Zhao, D.P., Kido, Y., Shukuno, H., 2002. Hot fingers in the mantle wedge: new insights into magma genesis in subduction zones. *Earth and Planetary Science Letters* 197, 105–116.
- Vlastélic, I., Staudacher, T., Semet, M., 2005. Rapid change of lava composition from 1998 to 2002 at Piton de la Fournaise (Réunion) inferred from Pb isotopes and trace elements: evidence for variable crustal contamination. *Journal of Petrology* 46, 79–107.
- Wegler, U., Lühr, B.-G., Snieder, R., Ratdomopurbo, A., 2006. Increase of shear velocity before the 1998 eruption of Merapi volcano Indonesia. *Geophysical Research Letters* 33, L09303.
- West, M.E., this issue. Recent eruptions at Bezymianny volcano—a seismological comparison. *Journal of Volcanology and Geothermal Research* XX, XX–XX.